Journal of Sound and Vibration (2001) **244**(3), 555–562
doi:10.1006/jsvi.2000.3503, available online at http://www.idealibrary.com on IDEAL®

LETTERS TO THE EDITOR

PRINCIPAL PARAMETRIC RESONANCE ZONES OF A ROTATING RIGID SHAFT DRIVEN THROUGH A UNIVERSAL JOINT

A. J. MAZZEI JR

Department of Mechanical Engineering, Kettering University, 1-709, 1700 *West Third Avenue, Flint, MI*, 48504-4898, *U.S.A.*

AND

R. A. SCOTT

*Department of Mechanical Engineering, The University of Michigan, G*044 *W. E. Lay Automotive Laboratory*, 1231 *Beal Avenue, Ann Arbor, MI*, 48109-2121, *U.S.A.*

(*Received* 6 *October* 2000)

1. INTRODUCTION

In reference [1], two models were developed for the motion of a driven shaft coupled via a U-joint to a uniformly rotating driving shaft. In one model, the shaft was treated as rigid whereas in the other it was treated as flexible. Both models led to the prediction of flutter and parametric instabilities. It was found that for shafts of proportions of those for a truck, the only parametric instabilities arising in practical ranges of operation were due to the rigid body modes (the shaft bouncing on the support springs), so that shaft flexibility can be ignored. In reference [1] the results were obtained using the monodromy matrix technique which is very computational intensive and number specific, so that parametric studies are very time consuming. In this note, some analytic expressions are developed for computing the principal parametric resonance zones using the methodology of Hill's infinite determinant. These expressions are used to determine the minimum amount of damping required to move the principal parametric zones out of the practical torque-rotational speed range. Note that a similar rigid body model was given by Iwatsubo and Saigo [2]. They also presented parametric studies on the influences of stiffness and damping, but no simple analytical approximations such as the ones at hand were presented. Moreover, the question of what value(s) of damping leads to driving the instabilities out of the practical range was not addressed.

2. EQUATIONS OF MOTION

Shown in Figure 1 is a shaft AB (length l) driven through a U-joint by a shaft BC which is rotating at a constant angular velocity Ω about its axis Z. (XYZ is an inertial set of axes).

The linearized equations of motion for the driven shaft were shown in reference [1] to be, for the case of zero initial angles between the driving and driven shafts,

$$v^2\begin{Bmatrix}\ddot{\gamma}\\ \ddot{\beta}\end{Bmatrix} + v\begin{bmatrix}\tilde{C}_y & \eta v\\ -\eta v & \tilde{C}_x\end{bmatrix}\begin{Bmatrix}\dot{\gamma}\\ \dot{\beta}\end{Bmatrix} + \begin{bmatrix}\tilde{K}_y & 0\\ 0 & \tilde{K}_x\end{bmatrix}\begin{Bmatrix}\gamma\\ \beta\end{Bmatrix} + \Gamma\begin{bmatrix}0 & 1\\ -1 & 0\end{bmatrix}\begin{Bmatrix}\gamma\\ \beta\end{Bmatrix} + \Gamma\sin(2\tau)$$

0022-460X/01/280555 + 08 $35.00/0

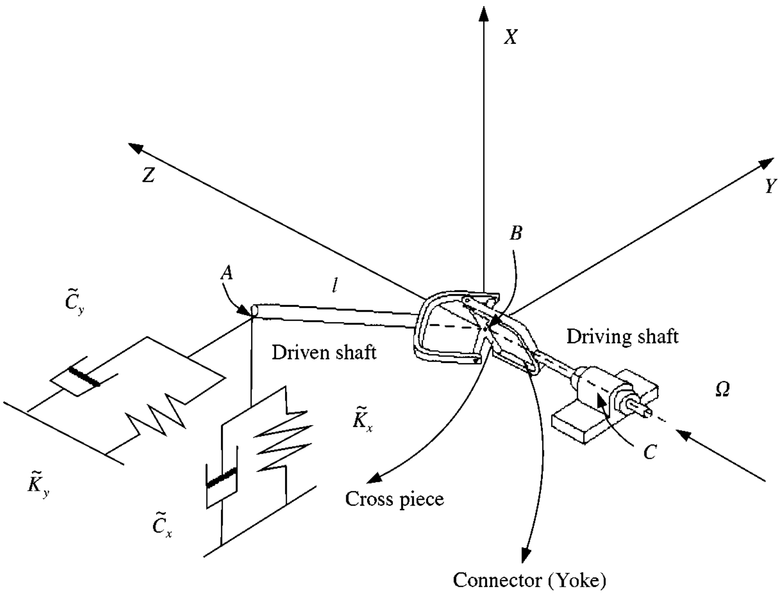

Figure 1. U-joint system.

$$\times\begin{bmatrix} -1 & 0 \\ 0 & 1 \end{bmatrix}\begin{Bmatrix} \gamma \\ \beta \end{Bmatrix} + \Gamma\cos(2\tau)\begin{bmatrix} 0 & 1 \\ 1 & 0 \end{bmatrix}\begin{Bmatrix} \gamma \\ \beta \end{Bmatrix} = \begin{Bmatrix} 0 \\ 0 \end{Bmatrix}, \tag{1}$$

where (1) γ and β are Euler angles, defined with respect to XYZ, specifying a body fixed frame; (2) v is a dimensionless rotational speed ($v = \Omega/\Omega_0$); for purposes of possible comparison with flexible models, Ω_0 is taken to be the first bending frequency of a non-rotating pinned–pinned beam, $\Omega_0 = (\pi^2/l^2)\sqrt{EI/\rho A}$ (here E denotes Young's modulus, I the area moment of inertia, ρ the mass density, and A the cross-sectional area); (3) the overdot stands for $\mathrm{d}/\mathrm{d}\tau$, $\tau = \Omega t$; (4) $\tilde{C}_x$, $\tilde{C}_y$, $\tilde{K}_x$, $\tilde{K}_y$ are dimensionless damping coefficients and springs rates given by $\tilde{C}_x = l^2 C_x/(J\Omega_0)$, $\tilde{C}_y = l^2 C_y/(J\Omega_0)$, $\tilde{K}_x = l^2 K_x/(J\Omega_0^2)$, $\tilde{K}_y = l^2 K_y/(J\Omega_0^2)$, $J = (m/12)(6R_o^2 + l^2) + m(l^2/4)$, where m denotes the mass of the shaft and R_o the outer radius of the shaft; (5) $\eta = J_{z,o}/J$, $J_{z,o} = mR_o^2$; (6) $\Gamma = T_0/(2J\Omega_0^2)$ (T_0 is the torque applied to the driving shaft BC).

For $\tilde{K}_y \neq \tilde{K}_x$ there are two principal parametric resonance zones (corresponding to motions in two planes). Using a one-term Hill-type expansion, the solutions can be approximated by

$$\gamma(t) = a_1\sin(\tau) + b_1\cos(\tau), \qquad \beta(t) = a_2\sin(\tau) + b_2\cos(\tau). \tag{2}$$

Inserting equations (2) into equations (1), using some trigonometric identities, and equating to zero the coefficients of $\sin(\tau)$ and $\cos(\tau)$, results in a system of linear homogeneous equations for a_1, b_1, a_2, b_2, the determinant of which must be zero, giving:

$$\begin{bmatrix} -v^2+\tilde{K}_y & -v\tilde{C}_y-\frac{1}{2}\tau & \frac{1}{2}\tau & -v^2\eta \\ v\tilde{C}_y-\frac{1}{2}\tau & -v^2+\tilde{K}_y & v^2\eta & \frac{3}{2}\tau \\ -\frac{3}{2}\tau & v^2\eta & -v^2+\tilde{K}_x & \frac{1}{2}\tau-v\tilde{C}_x \\ -v^2\eta & -\frac{1}{2}\tau & \frac{1}{2}\tau+v\tilde{C}_x & -v^2+\tilde{K}_x \end{bmatrix} = 0. \quad (3)$$

For $\tilde{K}_y = \tilde{K}_x = \tilde{K}$ and $\tilde{C}_y = \tilde{C}_x = \tilde{C}$, equation (3) can be written in the form of a cubic polynomial in Γ, the roots of which can be found by using MAPLE. Two of the roots are complex and one is real given by

$$\Gamma = \frac{v^2\tilde{C}^2 - 2\tilde{K}v^2 + \tilde{K}^2 - 2v^4\eta + 2v^2\eta\tilde{K} + v^4\eta^2 + v^4}{2v\tilde{C}}. \quad (4)$$

Equation (4) gives the stability boundary in (Γ, v) space of the principal parametric resonance zone (there is only one for $\tilde{K}_y = \tilde{K}_x$). It is in a form which can be readily used to perform parametric studies.

Note that there are problems for zero damping, a feature that was also seen in the monodromy matrix approach, where $\tilde{C} = 0$ led to flutter instabilities everywhere in (Γ, v) space. An issue, as in reference [1], is the extent to which the results for small values of $\tilde{C}$ are reasonable. Before investigating this further, the accuracy of equation (4) was checked by comparison with the exact monodromy matrix method. Shown in Figure 2 is a comparison for the case of a hollow shaft of truck proportions. The following parameter values are used: $l = 8{\cdot}96 \times 10^{-1}$ m, $\rho = 7{\cdot}83 \times 10^3$ Kg/m^3, $E = 2{\cdot}07 \times 10^{11}$ N/m^2, $R_o = 3{\cdot}4950 \times 10^{-2}$ m (outer radius), $R_i = 3{\cdot}3300 \times 10^{-2}$ m (inner radius), $\Omega_0 = 1{\cdot}53 \times 10^3$ rad/s and $\eta = 4{\cdot}5542 \times 10^{-3}$. The spring rates are $K_x = K_y = 2{\cdot}50 \times 10^3$ N/m and the damping coefficients are $C_x = C_y = 25{\cdot}0$ N/(m/s). Excellent agreement is seen, lending confidence to the present one-term approximation.

An important question concerns the value of $\tilde{C}$ that leads to Γ_{min} (see Figure 2) being outside the practical region. At Γ_{min}, $\mathrm{d}\Gamma/\mathrm{d}v$, which can be determined from equation (4), is zero. On specifying $\tilde{K}$ and $\tilde{C}$, the value of v can be determined for which $\mathrm{d}\Gamma/\mathrm{d}v = 0$. Substituting this value of v into equation (4) gives Γ_{min}.

In changing $\tilde{C}$, the process can be repeated and in this fashion a plot of Γ_{min} versus $\tilde{C}$ can be constructed, which is shown in Figure 3 (in dimensional form).

In the absence of damping and flutter terms, the zones would emanate from the natural frequencies. Instead of the procedure just noted, a good approximation to the location of Γ_{min} can be obtained by neglecting the time-dependent coefficients and the antisymmetric matrix in equation (1) and setting the torque and rotational speed equal to zero, which leads to the matrix

$$\begin{bmatrix} -\frac{l^2C_y}{J} & 0 & -\frac{l^2K_y}{J} & 0 \\ 0 & -\frac{l^2C_x}{J} & 0 & -\frac{l^2K_x}{J} \\ 1 & 0 & 0 & 0 \\ 0 & 1 & 0 & 0 \end{bmatrix} \quad (5)$$

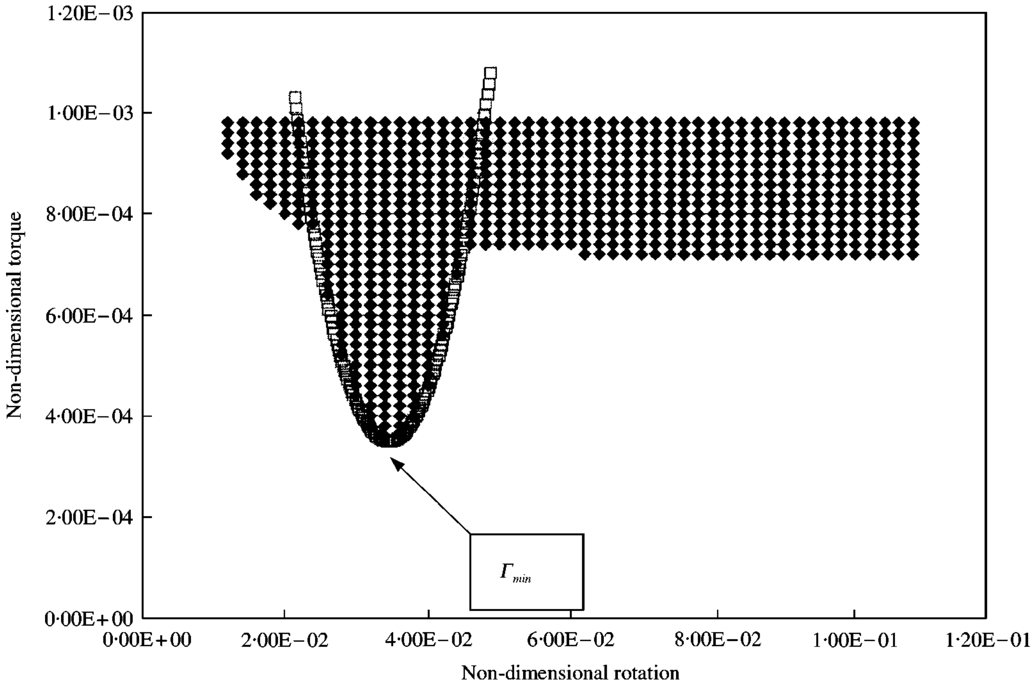

Figure 2. Region of instability for truck shaft and Γ_{min} (hashed zones given by monodromy method and boundary curve given by Hill's method).

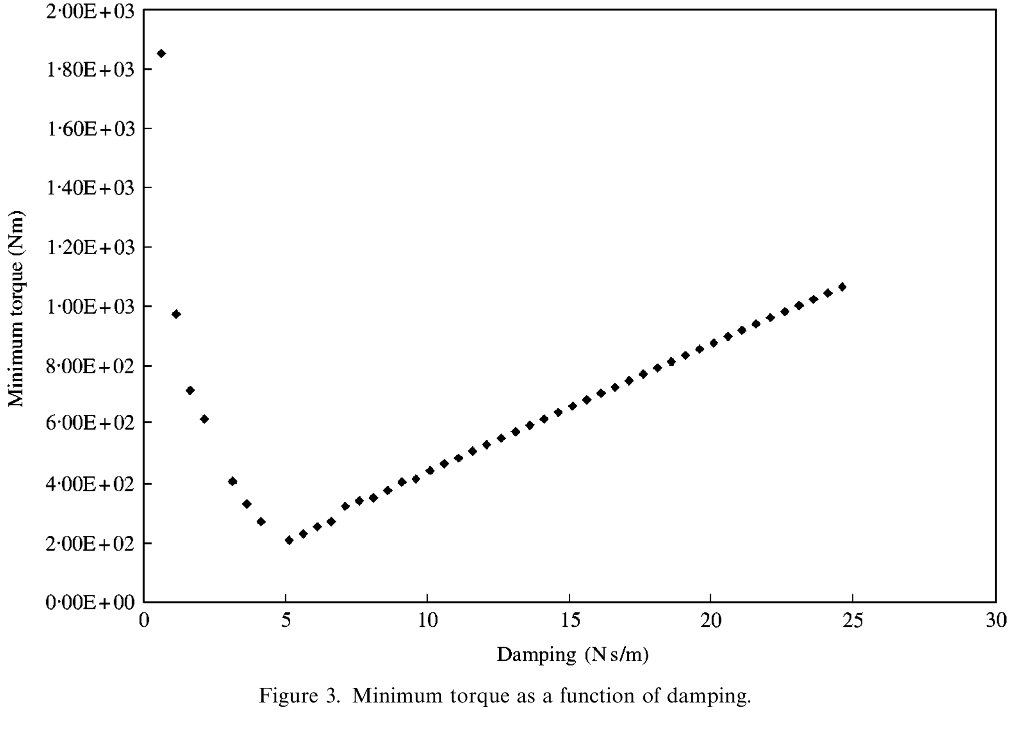

Figure 3. Minimum torque as a function of damping.

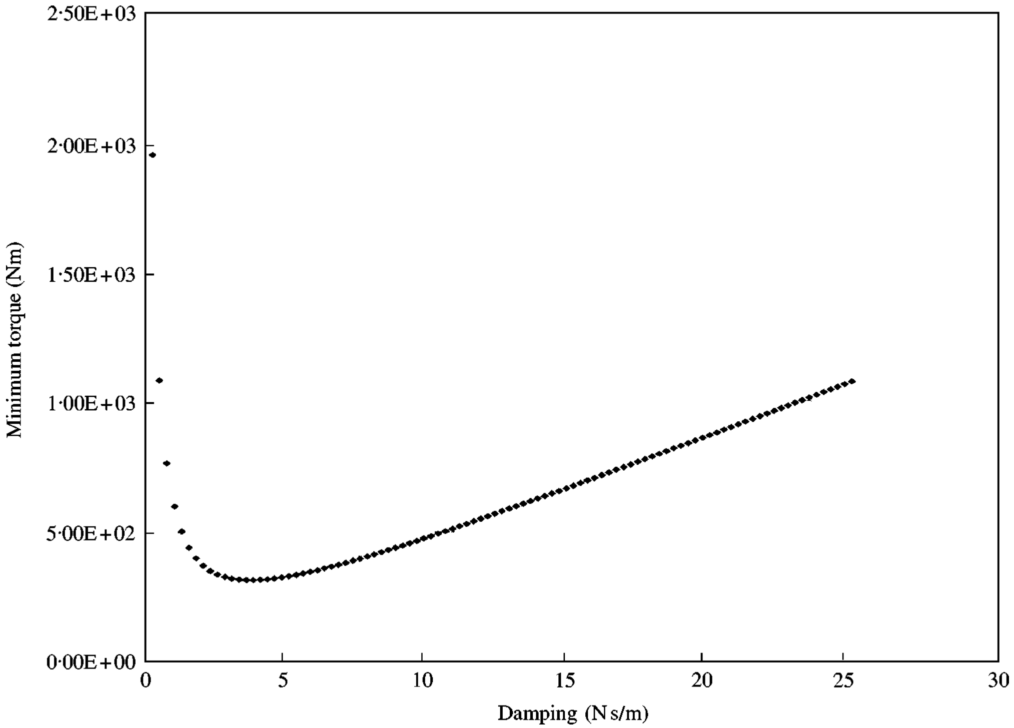

Figure 4. Minimum torque as a function of damping.

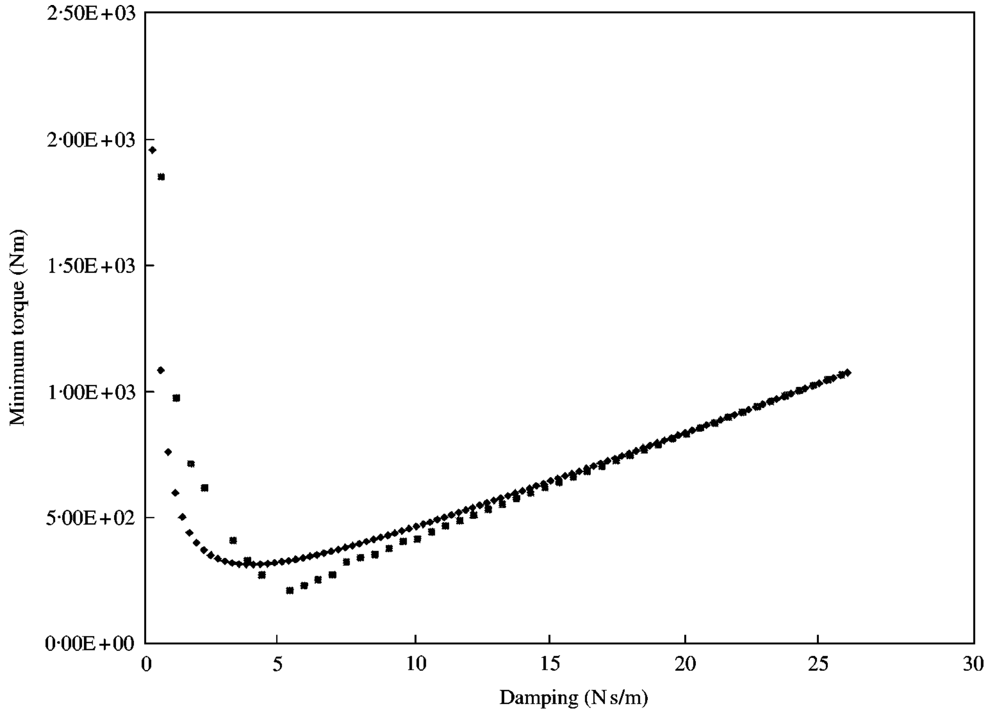

Figure 5. Comparison between approaches for obtaining minimum torque.

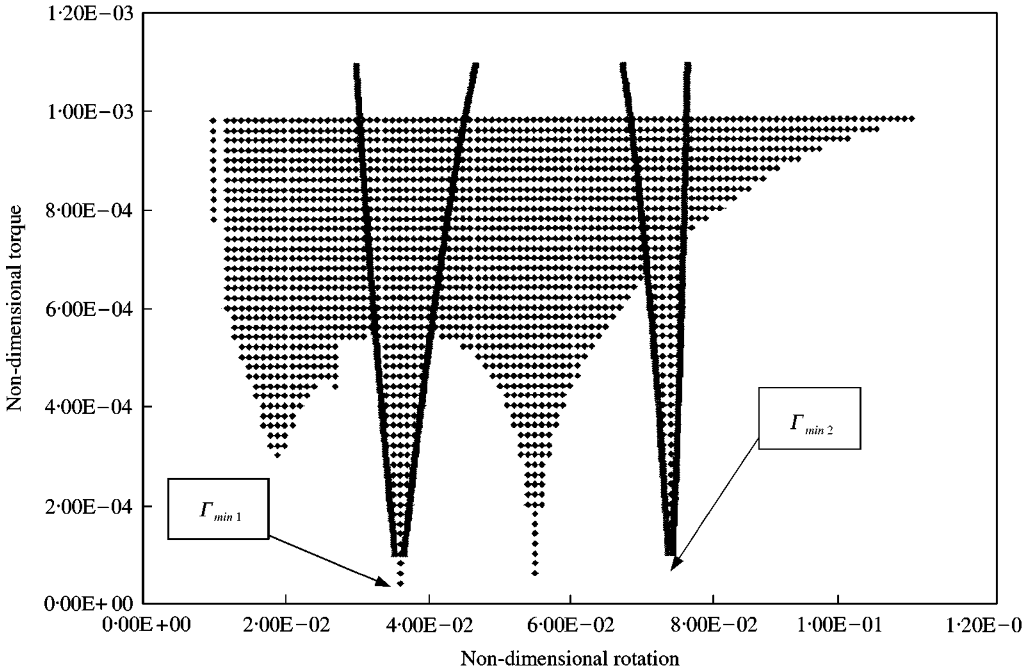

Figure 6. Comparison between principal regions of instability—monodromy matrix method (hashed region) versus Hill's method (lines).

Solving for the lowest eigenvalue of this matrix and substituting it into equation (4) leads to Γ_{min}. The results using this procedure are shown in Figure 4. In the practical range of rotation the eigenvalues do not vary significantly with rotational speed and so it was set equal to zero in the calculations. A comparison between the two approaches is shown in Figure 5. Good agreement is seen.

For very small values of $\tilde{C}$, the results are somewhat counterintuitive in that Γ_{min} is predicted to decrease with increasing values of C, a result which is connected to the presence of $\tilde{C}$ in the denominator of equation (4) and, presumably, the previous predictions [1] of flutter everywhere in the (Γ, v) space for $\tilde{C} = 0$. Inspection of Figure 3 shows that C_0 (values below which the problem starts) = 5 N s/m.

The associated value of Γ_{min} is 14% of the yield torque, which could be in the practical range of operation. As in reference [1], direct numerical integration of equation (1) subjected to certain specific initial conditions, and a logarithmic decrement procedure led to non-dimensional damping ratios $\zeta_1 = 0{\cdot}28$, $\zeta_2 = 0{\cdot}17$ (associated with γ and β respectively). Thus, for designs in which $K_x = K_y$, to avoid flutter and parametric resonance problems dampers would have to be provided to achieve the relatively high value of 0·28.

For $K_x \neq K_y$, the zones corresponding to vibrations in the XY and XZ planes are different and simple polynomial expressions such as equation (4) cannot be found. Instead, equation (3) is tackled directly. On specifying K_x and K_y, equation (3) is solved (using MAPLE) to obtain Γ as a function of $\tilde{C}$ and v. Shown in Figure 6 are the results obtained using the one-term approximation and the monodromy matrix technique. The parameters used here are $K_x = 2{\cdot}50 \times 10^3$ N/m, $K_y = 1{\cdot}06 \times 10^4$ N/m and $C_x = C_y = 5{\cdot}0 \times 10^{-1}$ N/(m/s) (the corresponding damping ratios are approximately $\zeta_1 = 0{\cdot}007$ and $\zeta_2 = 0{\cdot}003$). The first zone corresponds to the YZ plane and the second to the XZ plane. Again, excellent

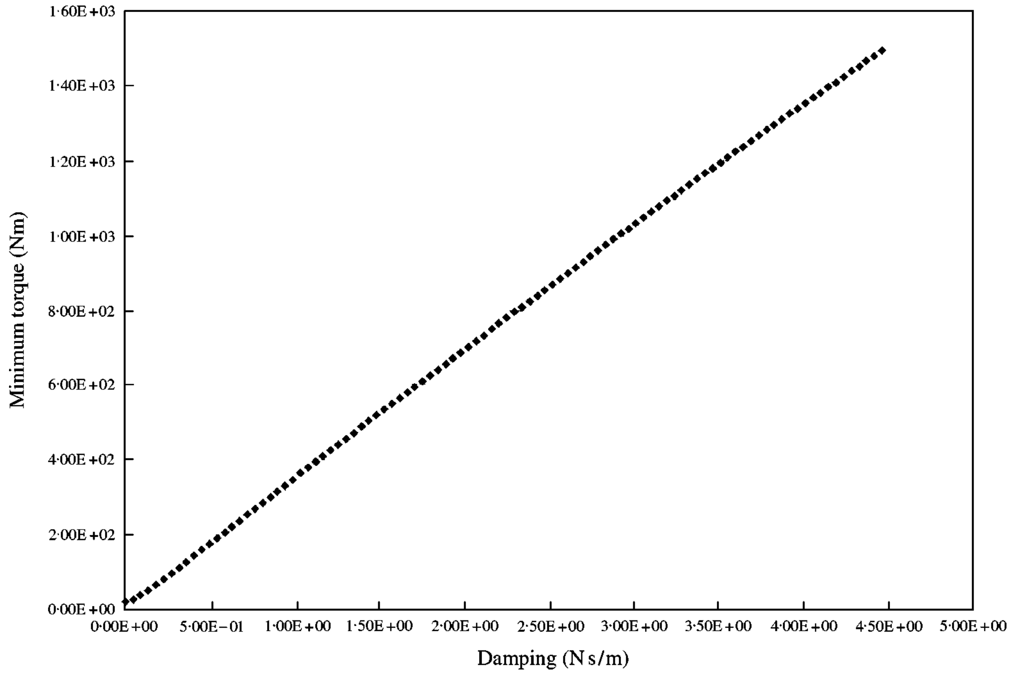

Figure 7. Γ_{min1} as a function of damping.

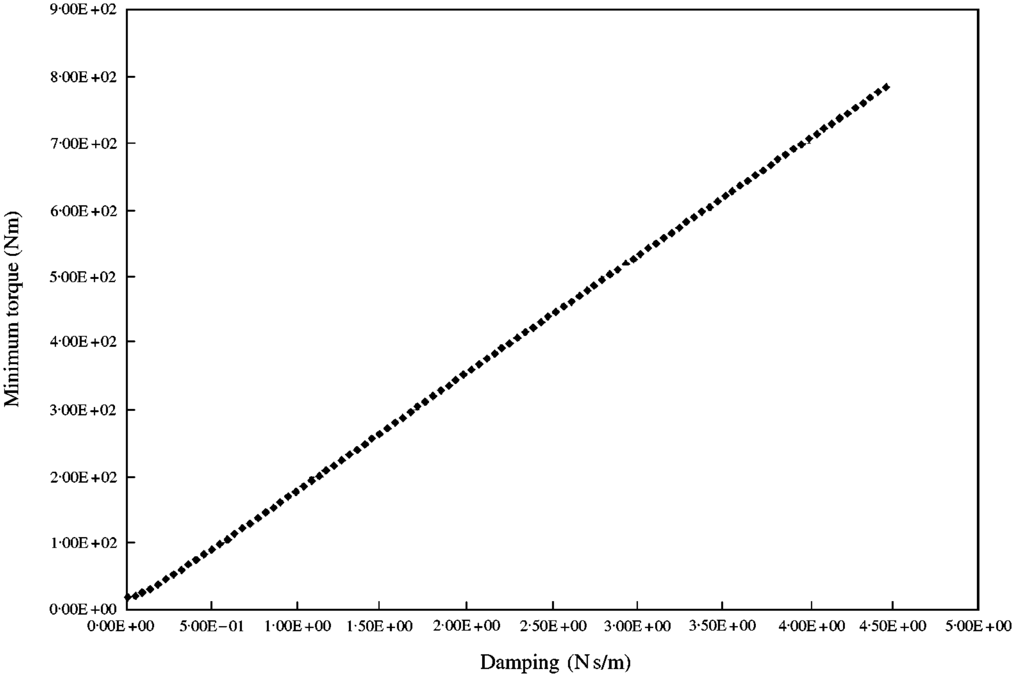

Figure 8. Γ_{min2} as a function of damping.

agreement is seen. Good estimates for Γ_{min1} and Γ_{min2} can be readily obtained using the approximation noted above, namely, substituting the lowest eigenvalues in equation (3). Figures 7 and 8 show the resulting plots for Γ_{min1} and Γ_{min2} versus C respectively.

Note that the problem associated with Γ_{min} decreasing with damping, attributed to flutter, has to all intents and purposes disappeared. This is consistent with the results presented in Mazzei *et al.* [1] in which it was noted that for $K_x \neq K_y$ very small values of damping moved the flutter zones out of practical ranges. As noted also by Iwatsubo and Saigo [2], having $K_x \neq K_y$ has a stabilizing effect on the system.

If one regards the limit torque that the shaft should experience as being, for example, 40% of the static yield ($\Gamma_{min} = 0{\cdot}00020$, corresponding in dimensional terms to 620 Nm) as a bound on the practical range of operation, then from Figures 7 and 8 it is seen that $C = 3{\cdot}5$ N s/m (corresponding to $\zeta_1 = 0{\cdot}038$, $\zeta_2 = 0{\cdot}035$, associated with γ and β) moves both Γ_{min1} and Γ_{min2} out of the practical range of operation. This value of damping is very realizable in practice.

REFERENCES

1. A. J. Mazzei Jr, A. Argento and R. A. Scott 1999 *Journal of Sound and Vibration* **222**, 19–47. Dynamic stability of a rotating shaft driven through a universal joint.
2. T. Iwatsubo and M. Saigo 1984 *Journal of Sound and Vibration* **95**, 9–18. Transverse vibration of a rotor system driven by a Cardan joint.